

Article

Dielectric, Mechanical, and Thermal Properties of Crosslinked Polyethylene Nanocomposite with Hybrid Nanofillers

Nurul Iman Abdul Razak¹, Noor Izyan Syazana Mohd Yusoff², Mohd Hafizi Ahmad³, Muzafar Zulkifli^{4,*}
and Mat Uzir Wahit^{1,5,*}

¹ Faculty of Chemical and Energy Engineering, Universiti Teknologi Malaysia, Johor Bahru 81310, Johor, Malaysia

² Advanced Membrane Technology Research Centre (AMTEC), Universiti Teknologi Malaysia, Johor Bahru 81310, Johor, Malaysia

³ Institute of High Voltage and High Current, School of Electrical Engineering, Universiti Teknologi Malaysia, Johor Bahru 81310, Johor, Malaysia

⁴ Green Chemistry and Sustainability Cluster, Branch Campus, Malaysian Institute of Chemical and Bioengineering Technology, Universiti Kuala Lumpur, Taboh Naning, Alor Gajah 78000, Melaka, Malaysia

⁵ Centre for Advanced Composite Materials (CACM), Universiti Teknologi Malaysia, Johor Bahru 81310, Johor, Malaysia

* Correspondence: muzafar@unikl.edu.my (M.Z.); r-uzir@utm.my (M.U.W.)

Abstract: Crosslinked polyethylene (XLPE) nanocomposite has superior insulation performance due to its excellent dielectric, mechanical, and thermal properties. The incorporation of nano-sized fillers drastically improved these properties in XLPE matrix due to the reinforcing effect of interfacial region between the XLPE–nanofillers. Good interfacial strength can be further improved by introducing a hybrid system nanofiller as a result of synergistic interaction between the nanofiller relative to a single filler system. Another factor affecting interfacial strength is the amount of hybrid nanofiller. Therefore, the incorporation amount of hybridising layered double hydroxide (LDH) with aluminium oxide (Al₂O₃) nanofiller into the XLPE matrix was investigated. Herein, the influence of hybrid nanofiller content and the 1:1 ratio of LDH to Al₂O₃ on the dielectric, mechanical, and thermal properties of the nanocomposite was studied. The structure and morphology of the XLPE/LDH–Al₂O₃ nanocomposites revealed that the hybridisation of nanofiller improved the dispersion state. The dielectric, mechanical, and thermal properties, including partial discharge resistance, AC breakdown strength, and tensile properties (tensile strength, Young’s modulus, and elongation at break) were enhanced since it was influenced by the synergetic effect of the LDH–Al₂O₃ nanofiller. These properties were increased at optimal value of 0.8 wt.% before decreasing with increasing hybrid nanofiller. It was found that the value of PD magnitude improvement went down to 47.8% and AC breakdown strength increased by 15.6% as compared to pure XLPE. The mechanical properties were enhanced by 14.4%, 31.7%, and 23% for tensile strength, Young’s modulus, and elongation at break, respectively. Of note, the hybridisation of nanofillers opens a new perspective in developing insulating material based on XLPE nanocomposite.

Keywords: crosslinked polyethylene; hybrid filler; dielectric properties; mechanical properties; thermal properties; hybrid nanocomposite



Citation: Abdul Razak, N.I.; Yusoff, N.I.S.M.; Ahmad, M.H.; Zulkifli, M.; Wahit, M.U. Dielectric, Mechanical, and Thermal Properties of Crosslinked Polyethylene Nanocomposite with Hybrid Nanofillers. *Polymers* **2023**, *15*, 1702. <https://doi.org/10.3390/polym15071702>

Academic Editor: Markus Gahleitner

Received: 6 February 2023

Revised: 21 February 2023

Accepted: 22 February 2023

Published: 29 March 2023



Copyright: © 2023 by the authors. Licensee MDPI, Basel, Switzerland. This article is an open access article distributed under the terms and conditions of the Creative Commons Attribution (CC BY) license (<https://creativecommons.org/licenses/by/4.0/>).

1. Introduction

Polymeric materials have been well known for years as electrical insulating materials because they have good dielectric, mechanical, and thermal strength. Crosslinked polyethylene (XLPE) has the best insulation properties among polymeric materials. XLPE materials are not limited to low-voltage and medium-voltage cable application, but are also used in high-voltage and extra-high-voltage cables [1,2]. As the XLPE material is subjected to the degradation process caused by high voltage current, it is also exposed to mechanical

damage that would occur during installation or operation. Furthermore, the stress and continuous bending of insulating materials would initiate defects and reduce polymeric materials' durability [3]. Therefore, in addition to dielectric properties, the mechanical and thermal properties of XLPE materials need to be studied to increase its service life by adding nanofiller into XLPE.

Starting with macro-sized fillers, progress in the field has allowed for the expansion to nano-sized fillers. The advantage of nano-sized filler is the high aspect ratio, resulting in high surface area, which can potentially change the property to enhance the insulation system [4]. To utilise the nano-sized filler's characteristics, uniform distribution of nanofiller into the XLPE matrix needs to be achieved by increasing the interfacial interaction between XLPE–nanofiller and internanofiller. The introduction of a hybrid nanofiller can achieve a robust interfacial bonding compared to a single filler system that is attributed to synergistic effect [5], and this process enhanced the mechanical behaviour of the XLPE nanocomposites [6] in addition to dielectric and thermal properties [7]. The properties of hybrid nanocomposite improved in dielectric properties and thermal conductivity in addition to promoting mechanical properties on Young's modulus and tensile strength [3,8–10] and showed remarkable performance with a homogeneous distribution of hybrid nanofiller obtained at low nanofiller loading with a maximum of 1 wt.% [11–13]. These successful studies proved that a combination of two different background characteristics achieve synergistic effect towards the nanocomposite with high compatibility achieved between matrix–nanofiller and interfiller. The nanofillers support each other by bringing the nanotube to platelet [14], inserting the nanosheet into nanofiber [8], and the capability of the nanofiller to sit well with other nanofiller should be considered.

Among the best hybrid nanofiller system selections is layered double hydroxide (LDH). The success of LDH studies on flame retardant, biomedical, gas barriers, and anti-corrosion led to an expansion to electrical insulators [15]. LDH has appreciable thermal stability in improving heat dissipation by distributing the temperature more uniformly throughout the electric insulation cable to ensure the reliability and stability of the nanocomposite material [16–19]. Moreover, the layered silicate of LDH contributes to increasing most of the mechanical properties, including strength, modulus, and stiffness of nanocomposite. Furthermore, LDH treated with sodium dodecyl sulphate (SDS) would change the morphology, expand the interlayer distance, and allow the polymer to intercalate [20]. With all these advantages, LDH has high potential as an electrical insulator nanofiller to hybrid with aluminium oxide (Al_2O_3) to increase the dielectric, mechanical, and thermal properties of XLPE nanocomposites. The alumina (Al_2O_3) nanofiller is well known for its excellent thermal stability and mechanical properties, and its high surface area makes it suitable as a co-nanofiller [13]. Moreover, silane-treated Al_2O_3 promotes smooth dispersion state and thus improved compatibility between matrix–filler adhesion [21]. The tensile strength increased 100%; in addition, Young's modulus of the nanocomposite increased 208%, which contributed to higher stiffness of the nanocomposite resulting in restricting polymer chain mobility. One of the strongest reasons for increasing mechanical properties is the alkyl group of Al_2O_3 linked like-a-bridge between Al_2O_3 and polymer as $-\text{OCH}_3$ part of trimethoxyoctyl silane chemically bonded to Al_2O_3 while the octyl group forms a linkage with the polymer [22].

The hybrid system often exhibits excellent properties, which typically cannot be found in nature because of the unique characteristics of individual nanofillers compared to single nanofillers. Resner et al. [3] studied nanoplatelets–nanotube, whereas Mansor et al. [23] explored spherical–spherical of XLPE nanocomposite that focused on the water treeing phenomenon. Meanwhile, Jose and Thomas [22] researched nanoplatelets–spherical by investigating its mechanical and thermal properties. Most of the properties of hybrid nanofiller tend to increase due to the reinforcing effect and better distribution of hybrid nanofiller into XLPE matrix. Furthermore, the study found that nanotube and spherical nanofillers have a higher tendency to agglomerate at higher concentration (>5 wt.%) than the nanoplatelets, which are well distributed regardless of concentration. Consequently, the

hybridising of LDH- Al_2O_3 must be studied to investigate the synergistic effect that could enhance the dielectric, mechanical and thermal characteristics of the XLPE nanocomposite as insulation materials.

2. Materials and Methods

2.1. Materials

The low-density polyethylene (LDPE) with trade name “TITANLENE LDF265YZ” produced by Lotte Chemical Titan (M) Sdn. Bhd., Pasir Gudang, Malaysia was used as the host polymer. The magnesium nitrate hexahydrate ($\text{Mg}(\text{NO}_3)_2 \cdot 6\text{H}_2\text{O}$) and sodium hydroxide (NaOH) were provided by Fluka and Irganox 1010 from BASF (M) Sdn. Bhd., Pasir Gudang, Malaysia respectively. The aluminium nitrate nonahydrate ($\text{Al}(\text{NO}_3)_3 \cdot 9\text{H}_2\text{O}$), sodium dodecyl sulfate (SDS), and Al_2O_3 nanoparticles with average particle size of <50 nm (TEM) (CAS No.:1344-28-1), trimethoxyoctylsilane and dicumyl peroxide (DCP) with average density of 1.56 g/cm^3 were obtained from Sigma Aldrich, Petaling Jaya, Malaysia, whereas sodium carbonate (Na_2CO_3) was supplied by QReC (Asia), Rawang, Malaysia. The deionised water was used as a solvent for preparing all solutions. The chemicals and reagents used in this experiment were of analytical grade and used without further purification.

2.2. Preparation of LDH-SDS

The Mg/Al LDH was synthesised with a ratio of 2:1 by the coprecipitation method. The 0.05 mol $\text{Mg}(\text{NO}_3)_2 \cdot 6\text{H}_2\text{O}$ and 0.025 mol $\text{Al}(\text{NO}_3)_3 \cdot 9\text{H}_2\text{O}$ were dissolved in deionized water (50 mL) and denoted as solution A. Caustic solution was prepared using 0.1 mol NaOH and 0.05 mol Na_2CO_3 in 100 mL as solution B, and solution C was 0.05 mol SDS in 100 mL of dissolved deionised water. Solutions A, B, and C were vigorously stirred at room temperature during the preparation. Then, solution A was added drop by drop into solution B and dropwise into solution C, a process that took about 3 h. The solution pH was adjusted and maintained at $\text{pH } 10.5 \pm 0.5$. The solution was kept under continuous agitation for 18 h at 65°C . The solid sample was finally collected using centrifuge at 5000 rpm until it reached pH 7 by washing it with deionised water. The resultant powder was dried in an oven for 12 h at 90°C and grounded using mortar and pestle to obtain pure Mg/Al powders. The schematic structures of LDH are shown in Figure 1.

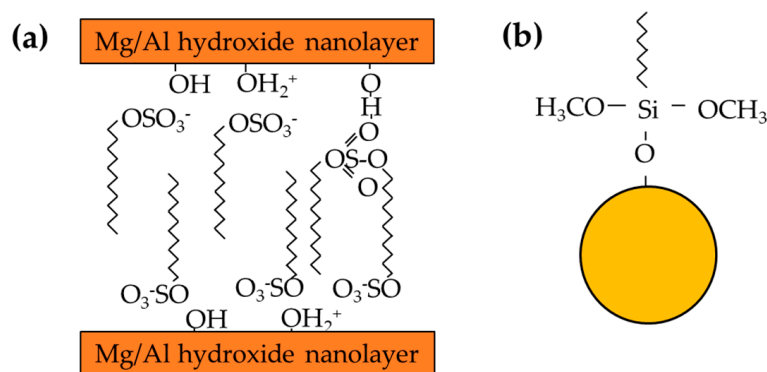


Figure 1. The structures of (a) LDH–SDS, (b) silane Al_2O_3 .

2.3. Surface Pre-Treatment of Al_2O_3

Approximately 11.52 g of Al_2O_3 was dispersed into 20:80 (water: 2-propanol) mixture solution at 2750 mL and treated with an ultrasonic bath for 15 min. To promote hydrolysis process, 25% ammonia solution is added in 61.2 mL to the suspension under vigorous stirring together with silane (64.8 mL). The reaction takes 24 h at room temperature and centrifuges at 5000 rpm for 7 min. The Al_2O_3 nanoparticles were dried at 80°C overnight, ground with a pestle and mortar to obtain the fine powder. The silane- Al_2O_3 treatment was adopted from Liu et al. [24] with the schematic structures of Al_2O_3 shown in Figure 1.

2.4. Preparation of Nanocomposite

Figure 2 illustrated the XLPE nanocomposite preparation by a melt mixing method using a Brabender internal mixer at 110 °C with a speed of 60 rpm in 7 min to obtain semi-XLPE. The formulation of XLPE nanocomposite is 0.0, 0.2, 0.5, 0.8, and 1.0 wt.% of hybrid LDH- Al_2O_3 nanofiller with a constant ratio of 1:1. All samples contained a composition of constant DCP and Irganox at 1.5 wt.% and 0.25 wt.%, respectively, throughout the preparation. The adding material sequence started with LDPE resin for about 2 min followed by LDH and Al_2O_3 at minutes 3 and 4, whereas DCP and Irganox were added later before completing 7 min and these parameters were constant during nanocomposite preparation. The fully crosslinked nanocomposites were obtained using hydraulic press, preheating the samples for 5 min at 120 °C without any pressure to flatten the sample for another 15 min at a temperature of 180 °C with 3.5 tons pressure. The samples were cooled down by cool-pressing for 15 min. All prepared samples were placed in a vacuum drying oven for the degassing process for 36 h at 80 °C prior to testing and characterisation analysis.

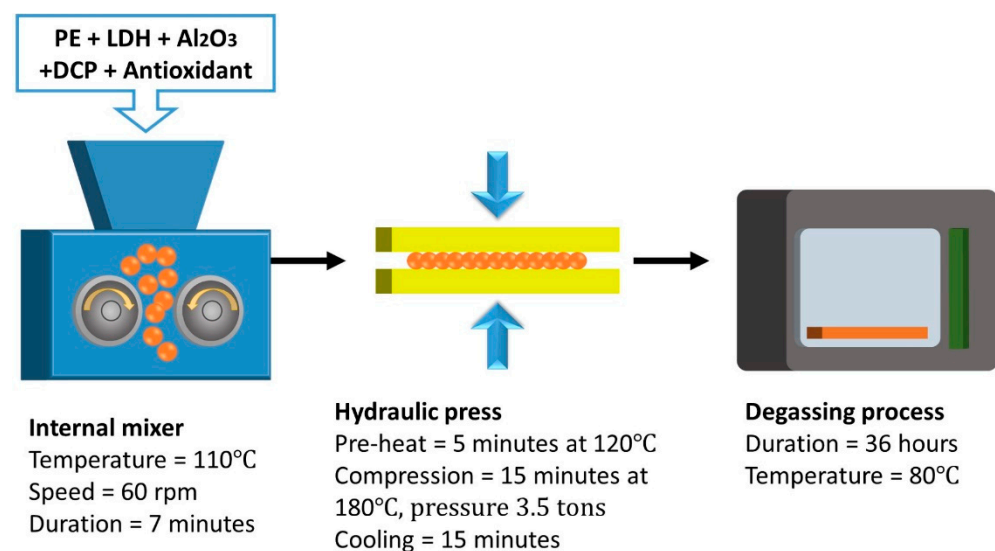


Figure 2. Schematic of the preparation of XLPE/LDH- Al_2O_3 nanocomposites.

2.5. Testing and Characterisation

The state of LDH nanofiller was studied using X-ray diffraction studies using a wide angle X-ray diffractometer (WAXD) with Ni-filtered $\text{CuK}\alpha$ source having a wavelength, $\lambda = 0.154$ nm operated at 40 kV and 30 mA with a step size of 0.02 from 2 thetas 1° to 10° (D8 Advance, Bruker AXS, Ettlingen, Germany). Fourier transform infrared spectroscopy (FTIR), Varian 4100 FTIR Excalibur Series instrument, in the attenuated total reflectance, attenuated total reflectance (ATR) mode, and the wavelength of ATR started in the range of $4000\text{--}400$ cm^{-1} , with 32 scans with a resolution of 4 cm^{-1} was used.

For the electrical test, the partial discharge (PD) measurements of the sample were conducted at the high voltage on the disc-like shape sample using a cylindrical-like high voltage electrode with 5 mm thickness of the ideal flat surface. According to the IEC 60270 standard, (a) 1 nF coupling capacitor and measuring impedance were connected parallel to the IEC (b) test containing the nanocomposite samples. The AC breakdown strength tests were conducted according to ASTM D149 standard by submerging the sample into silicon oil between two steel ball-bearing electrodes with a diameter of 6.35 mm. The 50-Hz AC voltage was increased gradually at a rate of 1 kV every 20 s to the sample until the sample experienced breakdown. Three samples were prepared with total points of 15 measurements collected at particular thicknesses for analysis. All the data were analysed using Weibull analysis.

The tensile properties include tensile strength, Young's modulus, and elongation at break carried out by Zwick with software test expert II at a crosshead speed of 50 mm/min

at 25 °C room temperature. The specimen dimensions are Type I according to ASTM D638, with a sample thickness of 3 mm. All measurements were conducted in five replicates, and the value was averaged.

The DSC tests were performed on Mettler Toledo STARe DSC 1 with samples sealed in aluminium pans under a nitrogen atmosphere of 5 mL/min in a temperature range between 25 °C to 300 °C at a heating rate of 10 °C/min. The heat of fusion, ΔH_m , was integrated with the DSC endothermic peak while crystallinity, X_c , normalised the heat of fusion to the heat of fusion of 100% crystalline PE ΔH_{mPE} as in Equation (1).

$$X_c = \frac{\Delta H_m}{\Delta H_{mPE}} \quad (1)$$

The specific enthalpy melting value for 100% crystalline PE was taken as 288 kJ/kg [25].

Morphological feature of the nanocomposite samples was analysed using Carl-Zeiss Supra 35VP FESEM. The fillers were nonconductive samples; thus, the sample needed to be coated in platinum using a platinum sputter coater under vacuum pressure for a time of 1 min at a current of 20 mA and voltage of 1.6 kV to provide electrical conductivity and prevent the surface charge accumulation. The nanocomposite samples were then examined at 10 kV of acceleration voltage.

3. Results

3.1. Characterisation of LDH Nanofiller

Figure 3a shows the XRD patterns of LDH and LDH-SDS. The diffraction peaks of LDH-SDS are shifted to the lower angle from LDH, indicating the intercalation of SDS. The peaks diffraction pattern is narrow and symmetrical, indicating a high degree of order in the LDH-SDS. The strong diffraction peaks (0 0 3), (0 0 6), and (0 0 9) at 2θ are 3.02°, 12.94°, and 19.49°, respectively, and the LDH-SDS interlayer distance is expanded to 2.923 nm from 0.772 nm of LDH. It is proven that SDS successfully intercalated the interlayer space of LDH. Moreover, a broad reflection in the range of 20°–23° (in the circle) confirmed that the hydrocarbon chains of SDS were intercalated into the interlayer of LDH. In general acknowledgement, the interlayer space is 2.6 nm as SDS anions intercalated into LDH [19].

Figure 3b shows LDH and LDH-SDS composition, and both showed a broad band at 3200 to 3400 cm^{-1} , indicating the stretching mode of hydroxyl group formation in the interlamellar water molecules and the brucite-like layers. The presence of SDS was confirmed by –CH stretching mode 2918, 2852 cm^{-1} , while the C–H bending mode band was at 1468 cm^{-1} . Meanwhile, the bending mode of the hydroxyl group appeared at 1656 cm^{-1} . The typical sulphate absorption bands stretch modes at 1216, 1000, 982, and 824 cm^{-1} . The absorption peak for carbonate 1378 cm^{-1} showed greater reduction at LDH-SDS than LDH, indicating SDS replaced carbonate anions into the interlayer [19,26]. The FTIR analysis was performed to certify that SDS was successfully intercalated into the interlayer.

Figure 3c highlights the FESEM morphology for nanofiller is nano-sized with a thickness of less than 30 nm (left) while the width ranges from 60 to 80 nm (right). Meanwhile, the TEM picture shows LDH was stacked one above the other in an orderly and tight manner by strong attractive force within anions interlayer in Figure 3d. This phenomenon was achieved due to a slow and homogeneous precipitation formed of LDH. After SDS ion intercalated inside the LDH nanolayer, the LDH was less orderly stacked on top of each other due to decreasing layers charges. This result has good agreement with XRD analysis.

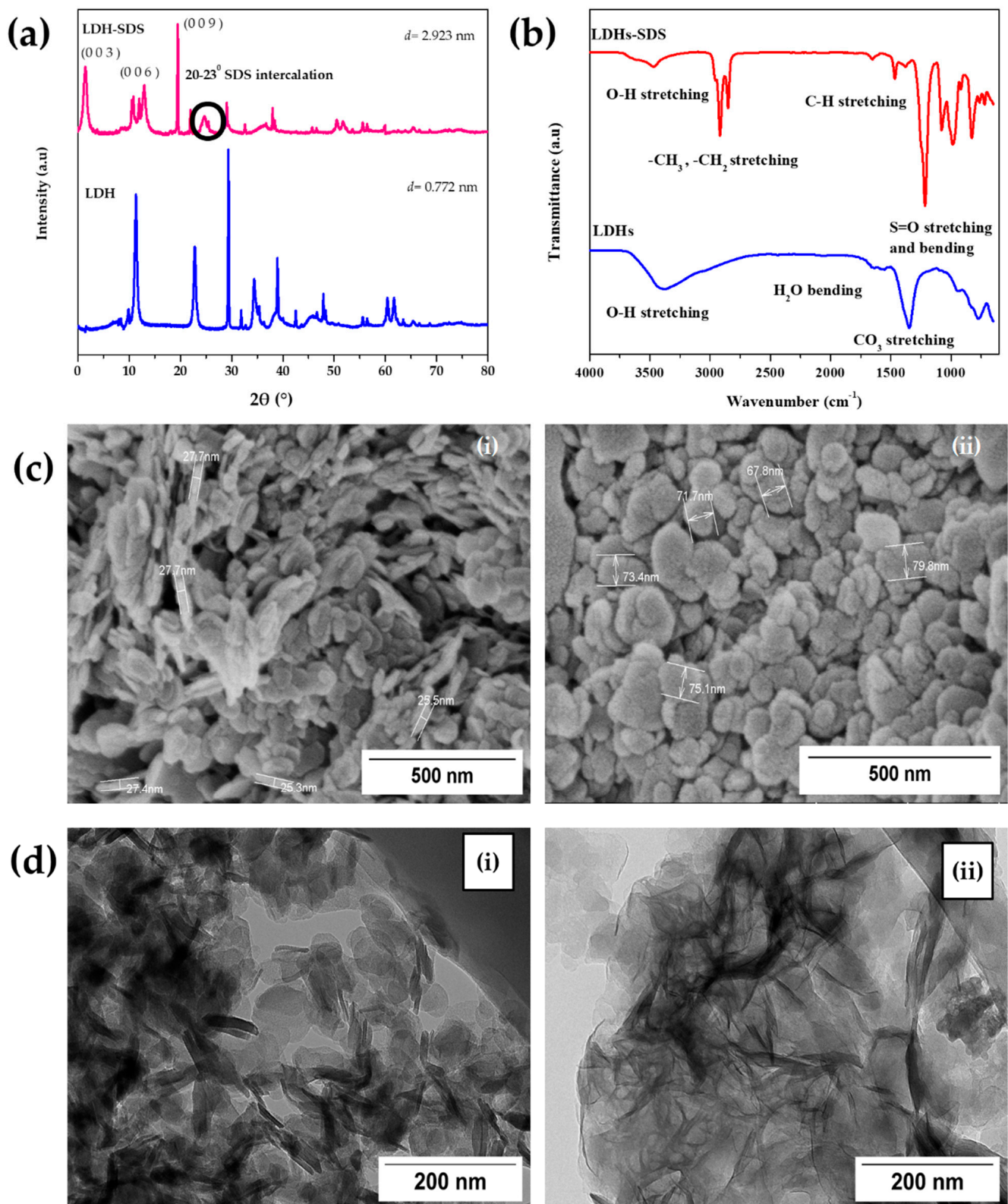


Figure 3. The nanofiller characterization on (a) XRD pattern of LDH and LDH–SDS, (b) FTIR spectra of LDH and LDH–SDS, (c) FESEM image (i) LDH thickness and (ii) width, (d) TEM image of (i) LDH and (ii) LDH–SDS nanofiller.

3.2. Dielectric Properties of LDH- Al_2O_3 Nanocomposite

3.2.1. Partial Discharge Measurement

Figure 4 shows the comparison of the partial discharge inception voltage (PDIV) and partial discharge extinction voltage (PDEV) on XLPE nanocomposite acquired based on different nanofillers loading. Theoretically, the higher the values of PDIV and PDEV exhibit better-insulating material because it requires a higher voltage level to initiate and extinguish the PD activities. For all samples tested, the trend showed that the values of PDIV and PDEV obtained using cylindrical-shaped high-voltage electrodes exhibited the lowest value at 0.0 wt.%. Introducing LDH- Al_2O_3 nanoparticles into the XLPE matrix changes the insulating materials' PDIV and PDEV. Even though the difference in terms of PDIV and PDEV were not significant from one sample to another, it showed that the amount of fillers had slightly influenced the profile of voltage where the PD signals initiated and extinguished with the percentage of error ranging 0.001 to 0.051.

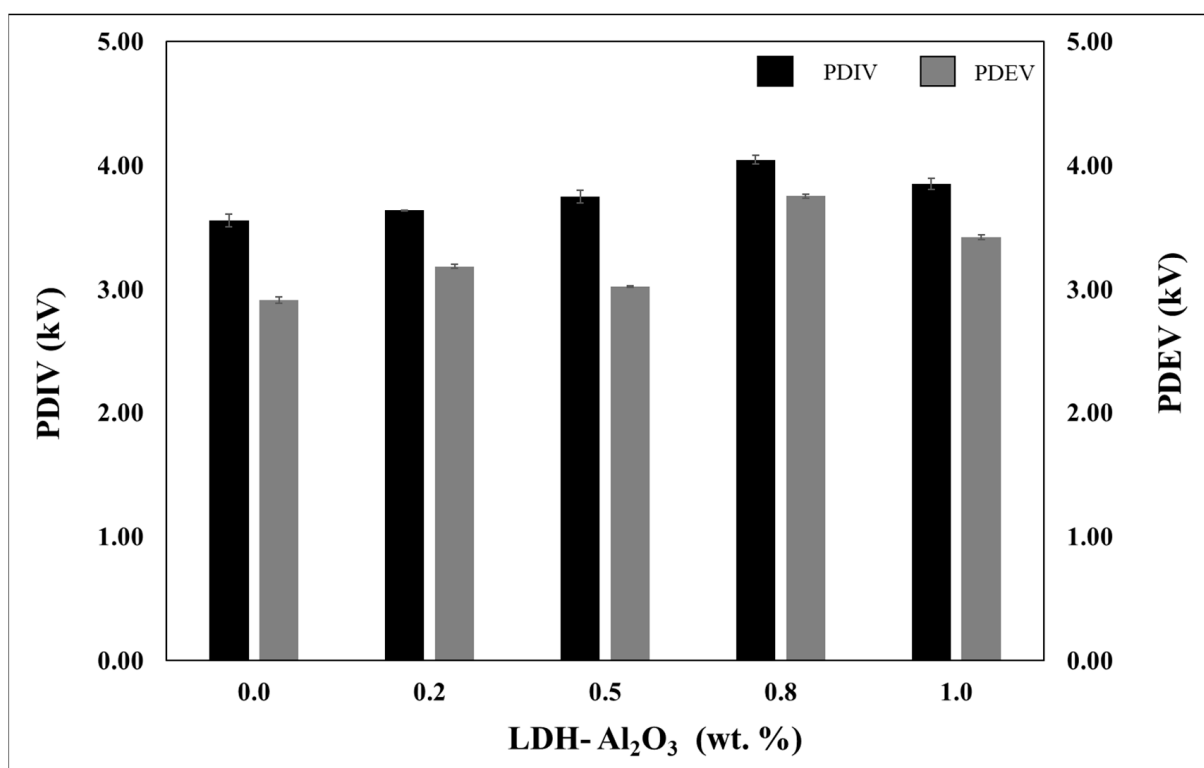


Figure 4. PDIV and PDEV of XLPE/LDH- Al_2O_3 nanocomposite.

The highest PDIV and PDEV was at 0.8 wt.% of the filler composition, followed by 0.5, 1.0, and 0.2 wt.%. It was related to the morphological analysis, which illustrated at 0.8 wt.% showed a uniform, smooth, and continuous surface compared to other nanocomposites. This outcome comprehensively reflected the morphological analysis results, which showed that the 0.8 wt.% sample has the largest and strongest interfacial region formed through the formation of interfacial bonds from the nanofillers-polymer surface interactions. At high voltage stresses, the values of PDIV and PDEV are relatively related to the distribution of the electric field on the sample. The effective deep trap is when interfacial region formation is large and strong enough to trap the charges that emitted from the high voltage source. Thus, less agglomeration of nanoparticles would form larger and stronger interfacial regions, which lead to a more effective mechanism in capturing charges [27]. As a result, it may reduce the charge mobility [28], hence reducing the charge transfer rate from the high voltage source to the XLPE nanocomposites under high voltage stress. The results obtained show that the electric field distributed at 0.8 wt.% is better than the other samples due to

the minimal local electric field distortion at 0.8 wt.% sample. It seems promising in PD resistance since the values of PDIV and PDEV increase.

Figure 5 shows the phase-resolved partial discharge (PRPD) pattern with the peak charge magnitude for all the PD pulses represented in every single dot. The pattern is asymmetrical on the applied voltage's positive and negative half cycles. The positive PD pulse count showed it was higher than the negative pulse count for all samples. The PD pulses were captured in the first quadrants, which depicted the phase angle from 0° to 90° , and the third quadrants, which indicated the phase angle from 180° to 270° also represents the discharge that happened on the sample's surface [29]. The PRPD pattern for all samples tested demonstrated that the type of PD that occurred was surface discharge, which refers to the 50 Hz voltage waveform. The discharge occurred on the surface of samples directly contacted with high voltage electrodes, which is indicated by the characteristics of the charge emitted through the PD activities. The maximum PD charges were extracted and are presented in Figure 6 accordingly.

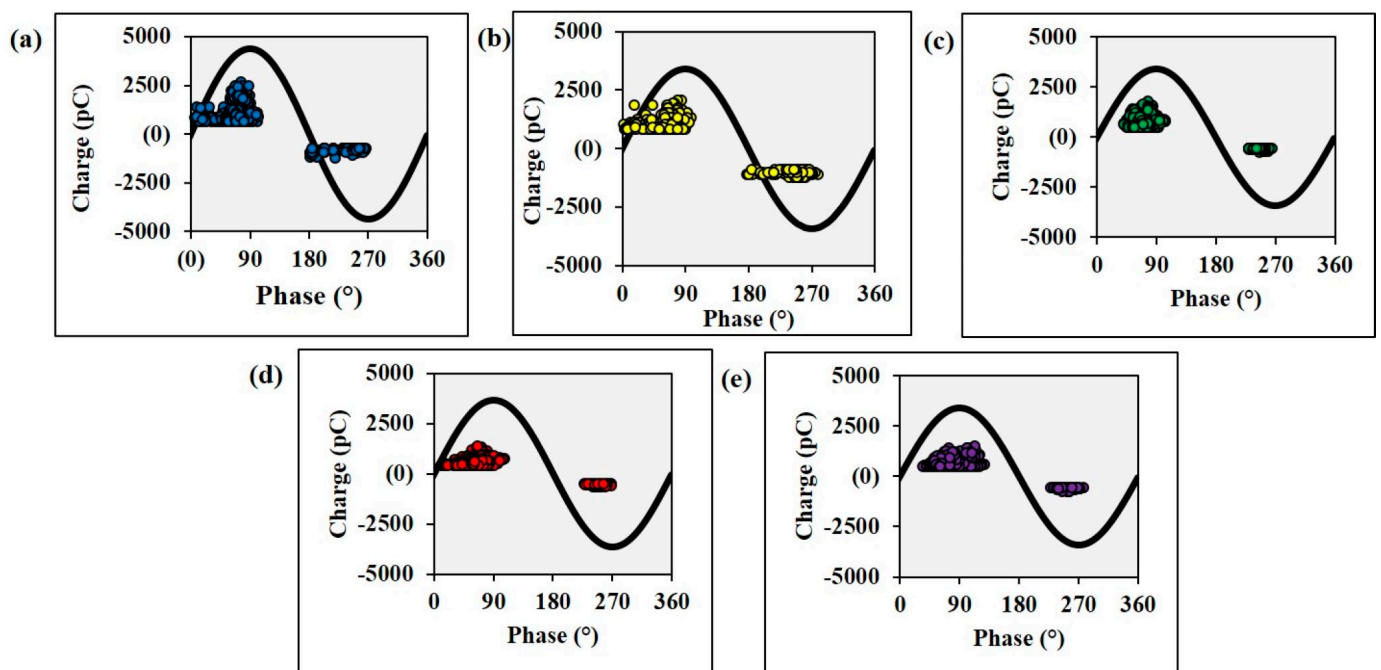


Figure 5. PRPD patterns of the XLPE/LDH–Al₂O₃ nanocomposites at (a) 0.0 wt.% (b) 0.2 wt.% (c) 0.5 wt.% (d) 0.8 wt.% and (e) 1.0 wt.%.

Figure 6 shows the maximum positive and negative PD magnitude released from the PD activities that occurred on the XLPE nanocomposites at different weight percentages of LDH–Al₂O₃ nanoparticles. The presence of LDH–Al₂O₃ nanoparticles within the XLPE matrix affected its PD resistance, which was stressed under a high electric field. Apparently, the PD magnitude has changed in each XLPE nanocomposite formulation. The PD magnitude is considered one of the comprehensive parameters in interpreting PD activities. Hence, this parameter is taken into account in determining the PD resistance for different XLPE nanocomposite formulations. The highest PD magnitude released from the PD activities was shown on the unfilled XLPE with 2656 pC positive charge magnitude. Moreover, the highest negative PD charge was exhibited by the PD activities that occurred on the unfilled XLPE with 1245 pC of charge emitted. The non-existent hybrid nanofiller appears to be least resistant against PD attacks, as shown by the highest charge produced compared to the XLPE nanocomposite.

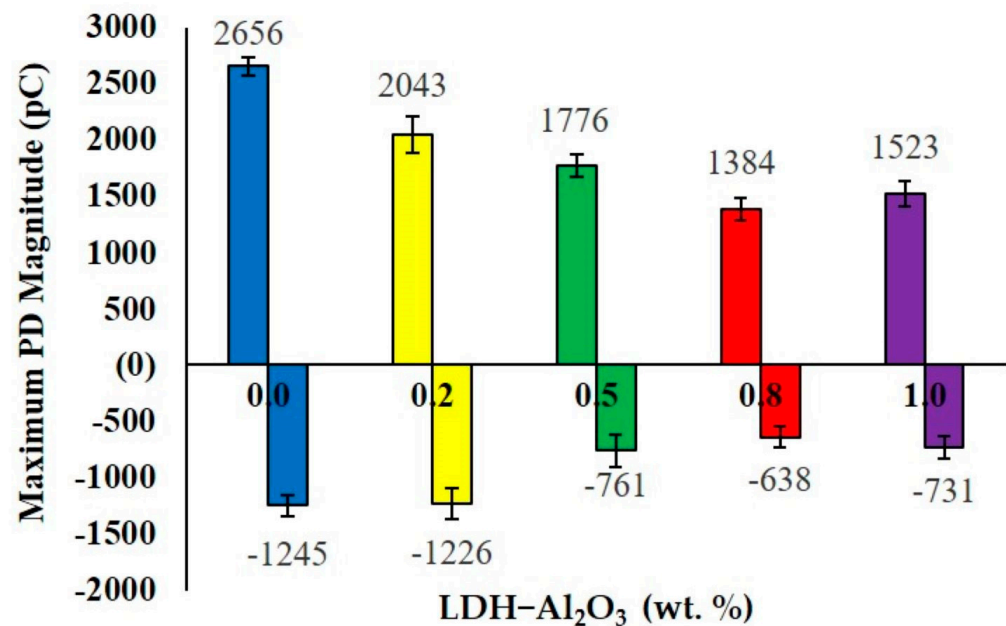


Figure 6. The comparison of maximum PD magnitude of XLPE/LDH–Al₂O₃ nanocomposites at varying the weight percentage of nanofillers.

Meanwhile, at 0.2 wt.%, the PD magnitude reduced to 23%. With further addition of 0.5 and 0.8 wt.% LDH–Al₂O₃ nanofillers, the PD magnitude has gradually decreased, recorded at 1776, –761 pC and 1384, –638 pC for positive and negative PD magnitude, respectively. Furthermore, 0.2 and 0.5 wt.% were considered insufficient weight percentages of nanofillers due to poor interfacial region, and the charge capturing mechanism tends to be less effective as the samples are stressed under a high electric field. Thus, the PD resistance was not significantly affected because the charges released from the external electrical sources were easy to move around on the sample’s surface and formed ionised channels.

The most effective loading occurred at 0.8 wt.% since it showed the lowest PD magnitude compared to the other weight of nanofillers. This result agreed with the outcomes from the FESEM analysis that showed 0.8 wt.% was the optimum formulation of XLPE nanocomposites, exhibiting well-distributed nanofillers compared to 1.0 wt.% and higher intensity of interfacial bonds formed through the nanofiller–polymer surface interactions compared to 0.2 and 0.5 wt.%. Therefore, the formation of large and robust interfacial regions leads to 0.8 wt.% having higher PD resistance. Unfortunately, 1.0 wt.% led to a significant increase in the PD magnitude recorded at 1523 and –731 pC. These results were due to the occurrence of increased nanofiller loading in the XLPE matrix. Higher filler concentration contributed to space charge trapping that occurred in XLPE, which became bigger [29]. The poor distribution of the nanoparticles is attributable to the incompatible interfaces between nanoparticles and polymer matrix, which eventually lead to the larger PD magnitude.

The addition of nanofillers in the XLPE nanocomposites create a wall by nano-sized filler arrangements in the host polymer, and it performed as a resistance to electron flow between two electrodes during the electrical stress. Therefore, it has been indicated that the XLPE sample with nanofillers had better PD-resistant insulation than the unfilled XLPE. The nanofillers serve as a barrier on the surface sample against PD attack. An indication supported by [30] confirmed that the addition of nanofillers enhanced the ability of XLPE nanocomposites to withstand surface degradation due to PD. Furthermore, the PRPD results show that the occurrences of PD pulses at 0.8 wt.% is the optimum amount of LDH–Al₂O₃ nanoparticles to incorporate in the XLPE matrix.

Figure 7 shows results obtained from PD numbers for XLPE nanocomposite. The number of PD pulses was 38751 for the unfilled XLPE, indicating the highest number

of PD pulses compared to other XLPE nanocomposite samples. The PD numbers were reduced using 5.7, 8.6, and 22.5% of unfilled XLPE as weight percentages of LDH- Al_2O_3 nanoparticles were filled in the XLPE matrix at 0.2, 0.5, and 0.8 wt.%, respectively. Then, the PD pulse count increased to 1.0 wt.% by 8.3% at 32764 and not more than 0.5 wt.% PD pulse count. It is clear that 0.8 wt.% showed the most effective formulation of XLPE nanocomposites with the lowest PD numbers, 30,027. The LDH- Al_2O_3 nanoparticles restricted the electron flow between two electrodes when the insulating materials were subjected to electrical stress. Therefore, the samples of XLPE with nanofillers have better PD resistance than the unfilled XLPE. Again, the nanofillers serve as a barrier on the surface sample against PD attack. These findings were supported by Awan et al. [30] and Chandrasekar et al. [31] who confirmed that the addition of nanofillers could enhance the ability of XLPE nanocomposites to withstand surface degradation due to PD. The trend of PD characteristics for PDIV, PDEV, PD magnitudes, and PD numbers have showed the same trend, which indicated that the most effective formulation was sample 0.8 wt.%, followed by sample 1.0 wt.%, and sample 0.5 wt.%. The unfilled sample showed the least resistance against PD attacks.

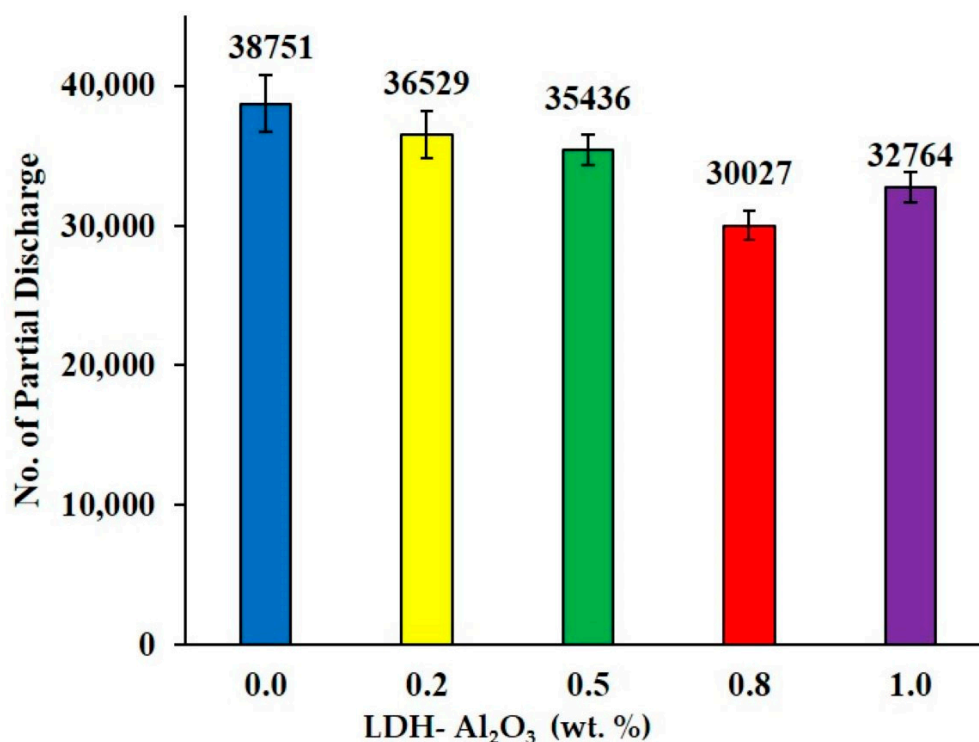


Figure 7. The total PD numbers of XLPE/LDH- Al_2O_3 nanocomposites at varying the weight percentage of nanofillers.

3.2.2. AC Breakdown Voltage

Figure 8 represents the Weibull probability plot comparing the AC breakdown strength of the XLPE nanocomposites containing 0.2 to 1.0 wt.% of LDH- Al_2O_3 nanoparticles. The 0.0 wt.% showed the lowest AC breakdown strength with 169.38 kV/mm. Introducing LDH- Al_2O_3 nanoparticles into the XLPE matrix increased the AC breakdown strength of the insulating materials. The breakdown strength increased to 180.50 kV/mm at 0.2 wt.% nanoparticles distributed into the XLPE matrix, which indicates an improvement of 6.6% from the non-existence of hybrid nanofiller; the AC breakdown strength of the nanocomposites of each loading of LDH- Al_2O_3 nanofillers increases as long it exists in the nanocomposites. It showed the enhancement of AC breakdown strength up to 11.8% and 15.6% at 0.5 and 0.8 wt.%, respectively. Through these improvements, it was found that the highest AC breakdown strength was 0.8 wt.% XLPE nanocomposites of LDH- Al_2O_3 nanoparticles

with 195.82 kV/mm, followed by 0.5 and 0.2 wt.% with 189.38 kV/mm and 180.50 kV/mm, respectively. However, the breakdown strength has slightly reduced to 173.97 kV/mm as the loading of hybrid nanofillers increased to 1.0 wt.%. The results align with the previous researchers, Said et al., who also found that the AC breakdown strength of XLPE has improved with the presence of nanoparticles within the XLPE matrix [32].

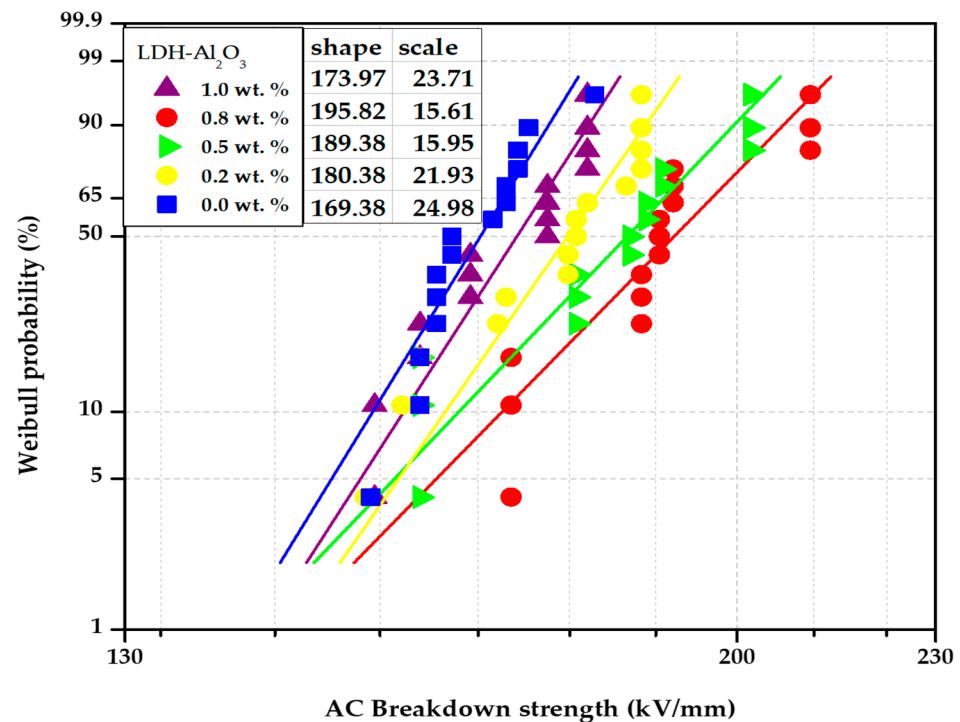


Figure 8. The Weibull analysis plot comparing the AC breakdown strength of XLPE/LDH-Al₂O₃ nanocomposites.

Based on these findings, the optimum loading was determined to be 0.8 wt.% with the highest AC breakdown strength. It could be due to the compatible nanofiller–polymer surfaces leading to improved filler distribution in XLPE matrices. It related to the distribution of LDH-Al₂O₃ nanoparticles within the XLPE matrix, which illustrated that 0.8 wt.% showed a smoother cross-section surface than other XLPE nanocomposites. The local electric field would be distributed more uniformly on the samples by forming interfacial bonds and better distribution of nanofillers [33], and the charges pulled under the influence of the electric field would be trapped on the interfacial regions. Therefore, charge mobility or charge transfer rate would reduce, as a result improving the AC breakdown strength of the XLPE nanocomposites [28].

From the results, the incorporation of LDH-Al₂O₃ nanoparticles has increased the AC breakdown strength, and this suggests that the nanoparticles act as electron scavengers in the insulation material under electrical stresses. The electron scavenger mechanism helps in capturing the fast electrons liberated from the external source, reducing the streamer propagation process and consistency [34]. Since the large interfacial regions between nanofillers–polymer contributed to increasing trap charge carriers and the ability to suppress electrons by being trapped on the nanoparticles surface, a reduction in mobility charge carriers occurred, thus improving the AC breakdown strength. The dielectric strength improved due to more time and energy needed to stimulate the charge carriers in forming conduction channels [35], as also highlighted by Montanari et al. [36]. The 1.0 wt.% were considered too high due to the shorter particle–particle distance at higher loading of hybrid nanofillers and tended to cause the nanoparticles to overlap and stick together via the attraction of van der Waals forces [37].

3.3. Tensile Properties of LDH- Al_2O_3 Nanocomposite

Table 1 shows the mechanical performance of XLPE/LDH- Al_2O_3 nanocomposite on tensile properties. The tensile properties are influenced by the content and distribution of incorporation LDH- Al_2O_3 nanofillers to XLPE matrix as well as interfacial interaction between XLPE and LDH- Al_2O_3 nanoparticles. The tensile strength, Young's modulus, and elongation at break initially increased and subsequently decreased as further addition of hybrid nanofillers to the XLPE matrix. It is reported in various studies that all samples of the nanocomposite have better tensile properties than unfilled XLPE [38–40]. This study ascertained an enhancement of tensile strength with increase in the LDH- Al_2O_3 nanofillers content from 0.0 to 0.8 wt.% and slight decrease at 1.0 wt.%. The reinforcing effect and a better dispersion are the main contributions that influenced the quality of the XLPE/LDH- Al_2O_3 nanocomposite tensile properties and the molecular chain bonds rarely broken [41].

Table 1. This mechanical properties of XLPE/LDH- Al_2O_3 nanocomposite.

LDH- Al_2O_3 (Wt.%)	Mechanical Performance of the Nanocomposite		
	Tensile Strength (MPa)	Young's Modulus (MPa)	Elongation at Break (%)
0.0	15.5 ± 0.7	140.8 ± 21.0	484 ± 16
0.2	16.9 ± 0.9	153.7 ± 12.6	510 ± 29
0.5	17.8 ± 0.4	174.3 ± 23.5	581 ± 15
0.8	18.1 ± 0.6	205.0 ± 16.6	633 ± 19
1.0	17.2 ± 0.8	180.4 ± 20.5	563 ± 18

It is intended that the amount of nanofillers reduce the free volume of the XLPE/LDH- Al_2O_3 nanocomposites as well as provide a well-distributed morphology and smoother fracture surfaces. The nano-sized particles provided a large interfacial interaction between LDH and Al_2O_3 to XLPE matrix. LDH is suggested to reduce the gaps between Al_2O_3 and is fairly connected through the matrix, which creates a network morphology [42]. Hence, LDH and Al_2O_3 nanoparticles were forming net structures in the XLPE matrix, improving the structural stability and enhancing the deformation resistance and shear resistance [40]. In the meantime, there was slight reduction in tensile strength at 1.0 wt.% but the value is still higher than 0.0 and 0.2 wt.% of XLPE/LDH- Al_2O_3 nanocomposites.

Meanwhile the enhancement in Young's modulus could be attributed to the synergistic stabilisation of LDH and Al_2O_3 that involves the formation of network morphology and the reinforcing effect of the LDH- Al_2O_3 on the nanocomposites. Lei et al. reviewed that hybrid nanocomposites, specifically from metal oxide and mineral fillers, have a much higher modulus than polymer matrices [43]. The addition of nanofillers increased the stiffness of the nanocomposite; consequently, Young's modulus also increased. The stiffness of the LDH- Al_2O_3 nanocomposites changed by crystallinity, which was observed from the DSC results. This improvement is attributed to the layer silicate structure of LDH, which mainly contributed to increasing Young's modulus due to high aspect ratio with large surface area as compared to Al_2O_3 nanofillers. As a result, the capability of stress transfer was higher across the reinforcement and nanocomposites; thus, the applied stress is disseminated by the interface more evenly [44]. Moreover, the tendency to interconnect and form a network structure of LDH is larger than in Al_2O_3 nanofillers [39].

The increasing of elongation at break values of XLPE/LDH- Al_2O_3 nanocomposites due to incorporation of a low number of nanoparticles into the nanocomposite improved the interaction between the molecules by slipping without breaking the samples due to the nanoparticles being reinforced and oriented along the stress direction resulting in higher elongation at breaks. However, further addition of LDH- Al_2O_3 nanofillers to the XLPE matrix subsequently increased the restriction of mobility on polymer chains; thus, the

elongation at break showed a decrement curve. Notably, this situation is expected in most polymer nanocomposites [32].

The small amount of LDH- Al_2O_3 nanofiller provides a huge total interface area and increases reinforcement efficiency. The reinforcing effect of the small amount of nanoparticle loadings has huge specific surface area and dramatically larger total interface area for reinforcement work efficiency. It is shown that, at lower weight percentage, the addition of LDH- Al_2O_3 nanofiller in XLPE matrix increases surface interaction bonding between the molecules. At the high amount of LDH- Al_2O_3 nanofiller, tensile properties showed a gradual drop. These experimental results are attributed to the reinforcing effect of the nanoparticles in which a higher number of nanoparticles reduces the reinforcing effect by the poor dispersion, agglomeration of nanoparticles, and large volumes of voids. These agglomerated nanoparticles occur due to the filler–filler interaction being higher than filler–matrix interaction and acting as stress concentration in nanocomposites. The slight volume of voids at the interface or trapped in a cluster would make the molecule move freely; thus, the polymer chains' mobility slipped past one another and later decreased the tensile performance [45].

Generally, the addition of nanofillers to most polymer nanocomposites is expected to reduce the values because of the restriction in chain mobility caused by poor interconnection between nanofillers and polymer chains [45]. However, the results obtained at 0.8 wt.% significantly increased the three key mechanical properties, for instance tensile strength, Young's modulus and elongation at break. The improvement in mechanical properties have been correlated with the surface fracture of nanocomposite in Figure 9. Moreover, as the nanofillers–matrix are located close to each other, the nanofillers surface needs higher temperature to induce the motion whereas the matrix which is unaffected with nanofillers surface properties is unchanged [46].

3.4. Morphology of LDH- Al_2O_3 Nanocomposite

Figure 9 shows cross-sectional morphologies of the XLPE/LDH- Al_2O_3 nanocomposite using FESEM. The nanocomposite displays good distribution and shows no obvious visible agglomeration of hybrid LDH- Al_2O_3 nanofiller at different weight percentages in XLPE to a large extent. From the cross-section, surface fracture of the nanocomposite showed the tendency of nanofillers to aggregate is low. This situation is explained by interfiller interaction being low compared to nanofiller–matrix interaction due to the different surface characteristics and different surface energies that belong to hybrid nanofillers. The FESEM images showed that hybrid nanofillers have great potential to resolve the agglomeration of nanofillers and the nanocomposite surface was observed to become rougher with the addition of hybrid nanofiller into XLPE nanocomposites.

3.5. Differential Scanning Calorimetry of XLPE/LDH- Al_2O_3 Nanocomposite

Table 2 provides the thermal performance of XLPE/LDH- Al_2O_3 nanocomposite based on crystallisation temperature (T_c), melting temperature T_m , enthalpy (ΔH_m), and crystallinity (X_c) of nanocomposite. Both T_m and T_c increased slightly as a result of nanofiller content of all nanocomposite samples. The T_m and T_c move toward the high temperature direction, from 107 °C to 109 °C and 90 °C to 94 °C, respectively, with the introduction of LDH- Al_2O_3 nanofillers. The temperature increment is due to increased interaction between the XLPE matrix and LDH- Al_2O_3 nanofillers, which lead from restricted mobility of XLPE chains to relaxation of the nanocomposite system at higher temperature. Another reason for increment of about 2 °C is attributed to the introduction of LDH- Al_2O_3 is that it provides better networking to improve thermal properties [47]. Donghe and Qingyue concluded the introduction of nanoparticles in XLPE showed two main parameters: first, an increase in the melting point; second, the ability of crystallisation to slow down due to restriction in movement of molecular chain segment [40,48].

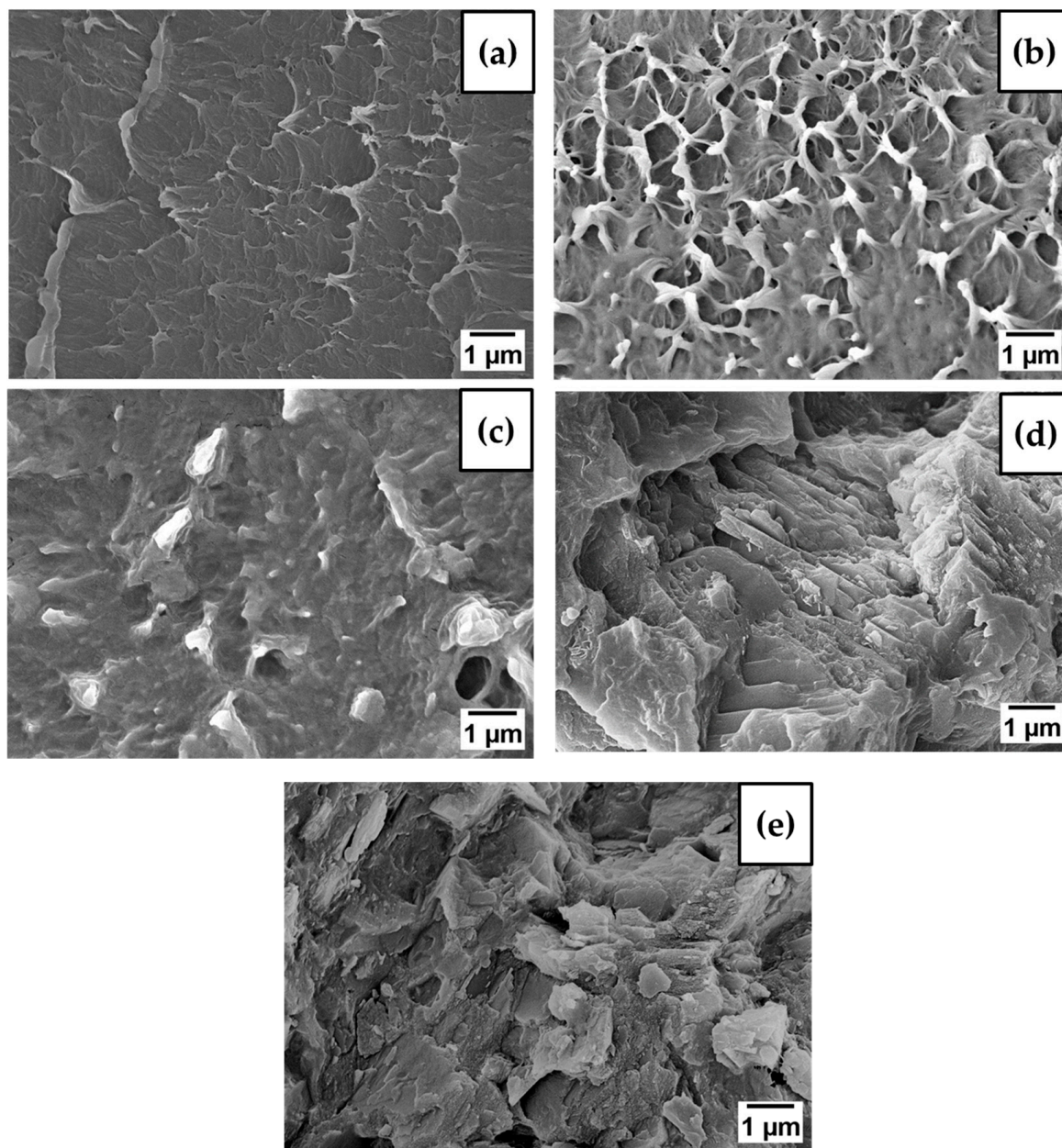


Figure 9. The FESEM image of XLPE/LDH- Al_2O_3 nanocomposite at (a) 0.0 wt% (b) 0.2 wt.% (c) 0.5 wt.% (d) 0.8 wt.% and (e) 1.0 wt.%.

Table 2. The DSC analysis of XLPE/LDH- Al_2O_3 nanocomposite.

LDH- Al_2O_3 (Wt.%)	Thermal Performance of Nanocomposite			
	Crystallisation Temperature (°C)	Melting Temperature (°C)	Enthalpy (J/g)	Crystallinity (%)
0.0	90.5	107.8	99.31	34.5
0.2	93.7	109.7	124.3	43.2
0.5	93.5	109.5	125.9	43.7
0.8	93.2	109.3	132.8	46.1
1.0	94.5	109.1	101.7	35.3

Based on DSC thermograms in Figure 10a,b, the endothermic recorded during the second heating cycle and the exothermic curve was recorded cooling from the melt of

the first heating cycle, respectively. The degree of crystallinity, which can be calculated using the melting enthalpy with the specific enthalpy melting value for 100% crystalline PE, was taken as 288 kJ/kg. Note that the slight increase in T_c and T_m from unfilled XLPE to XLPE nanocomposite ensures that the crystalline region melts and enhances mechanical properties at relative temperatures [49]. This finding is in agreement with Thomas et al. [50] stating that DSC results of XLPE nanocomposites had comparable results on T_c and T_m indicating a low effect of nanofillers on XLPE phase transformations. However, after analysing the value of the X_c , it can be seen that the incorporation of LDH- Al_2O_3 to XLPE caused the X_c to increase. It was also that with the addition of LDH- Al_2O_3 content, an explicit decrease in the X_c was observed but still higher than the unfilled XLPE [3].

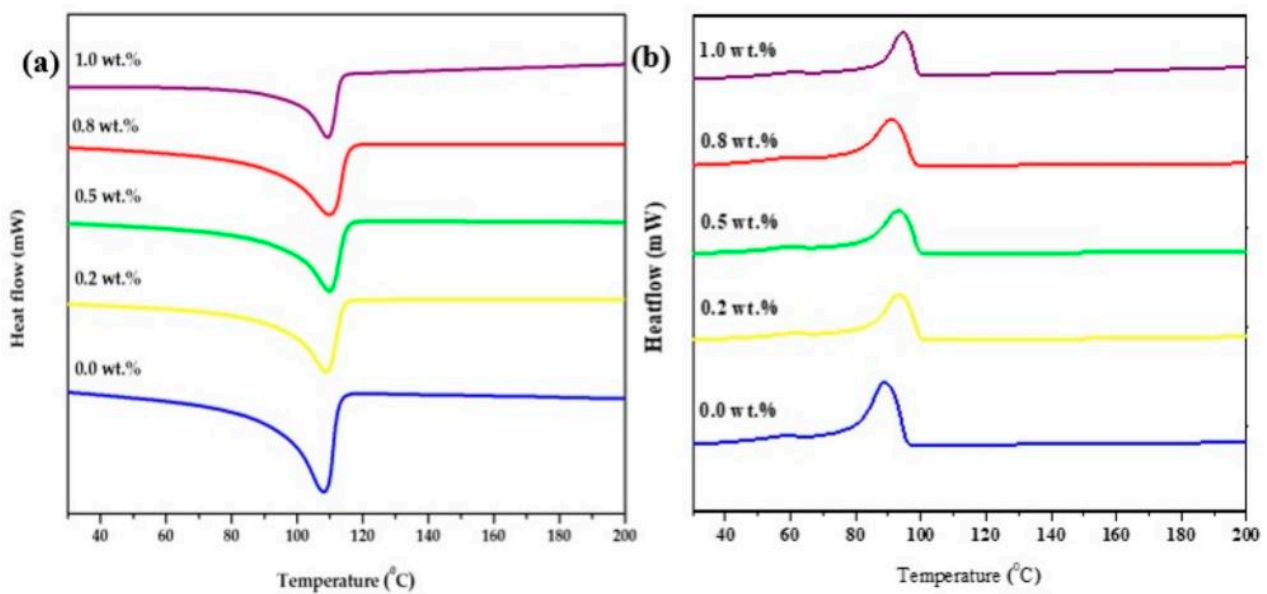


Figure 10. The DSC thermograms of XLPE/LDH- Al_2O_3 nanocomposites (a) 2nd heating cycle (b) cooling cycle.

4. Conclusions

The incorporation of hybrid LDH- Al_2O_3 nanofiller into XLPE matrix has successfully improved the dielectric properties of PD and AC breakdown voltage without sacrificing the mechanical properties of the nanocomposites. Based on the amount of hybrid nanofiller, the 0.8 wt.% showed the potential hybrid loading of XLPE/LDH- Al_2O_3 nanocomposites. The dielectric properties were enhanced, with PD magnitude reducing to +1384, −638 and the PD number being reduced to 30,027, whereas the mechanical properties exhibit the highest tensile strength, Young's modulus, and elongation at break of 18.1 MPa, 205 MPa, and 633%, respectively. Moreover, the formation of a strong inter-phase region was promoted by the balance effect of morphological features of the hybrid network of each component with no visible agglomeration. It was found that increasing the crystallinity slightly improved the thermal properties of the hybrid nanocomposite in this study. The outcomes of this work provide further guidance for the design of high-voltage direct current insulation materials.

Author Contributions: Conceptualization, M.U.W., M.H.A. and N.I.S.M.Y.; methodology, N.I.A.R.; validation, M.U.W. and M.H.A.; formal analysis, N.I.A.R.; investigation, N.I.A.R.; resources, M.U.W., M.H.A. and N.I.A.R.; data curation, M.U.W. and M.H.A.; writing—original draft preparation, N.I.A.R. and M.Z.; writing—review and editing, M.U.W., M.H.A., M.Z. and N.I.S.M.Y.; visualization, N.I.S.M.Y.; supervision, M.U.W. and M.H.A.; project administration, M.U.W. and M.Z.; funding acquisition, M.U.W. and M.Z. All authors have read and agreed to the published version of the manuscript.

Funding: This work was supported by UTM Fundamental Research Grant Scheme (UTMFR) no: Q.J130000.2551.20H68, Reference no: PY/2019/01755.

Institutional Review Board Statement: Not applicable.

Informed Consent Statement: Not applicable.

Data Availability Statement: The data presented in this study are available upon request from the corresponding author.

Conflicts of Interest: The authors declare no conflict of interest.

References

1. Haque, S.; Ardila-Rey, J.A.; Umar, Y.; Mas'ud, A.A.; Muhammad-Sukki, F.; Jume, B.H.; Rahman, H.; Bani, N.A. Application and Suitability of Polymeric Materials as Insulators in Electrical Equipment. *Energies* **2021**, *14*, 2758. [[CrossRef](#)]
2. Lv, H.; Lu, T.; Xiong, L.; Zheng, X.; Huang, Y.; Ying, M.; Cai, J.; Li, Z. Assessment of thermally aged XLPE insulation material under extreme operating temperatures. *Polym. Test.* **2020**, *88*, 106569. [[CrossRef](#)]
3. Resner, L.; Lesiak, P.; Taraghi, I.; Kochmanska, A.; Figiel, P.; Piesowicz, E.; Zenker, M.; Paszkiewicz, S. Polymer Hybrid Nanocomposites Based on Homo and Copolymer Xlpe Containing Mineral Nanofillers with Improved Functional Properties Intended for Insulation of Submarine Cables. *Polymers* **2022**, *14*, 3444. [[CrossRef](#)] [[PubMed](#)]
4. Niu, Y.; Wang, H. Dielectric nanomaterials for power energy storage: Surface modification and characterization. *ACS Appl. Nano Mater.* **2019**, *2*, 627–642. [[CrossRef](#)]
5. Charitos, I.; Georgousis, G.; Klonos, P.A.; Kyritsis, A.; Mouzakis, D.; Raptis, Y.; Kontos, A.; Kontou, E. The synergistic effect on the thermomechanical and electrical properties of carbonaceous hybrid polymer nanocomposites. *Polym. Test.* **2021**, *95*, 107102. [[CrossRef](#)]
6. Idumah, C.I.; Obele, C.M. Understanding interfacial influence on properties of polymer nanocomposites. *Surf. Interfaces* **2021**, *22*, 100879. [[CrossRef](#)]
7. Yao, J.; Hu, L.; Zhou, M.; You, F.; Jiang, X.; Gao, L.; Wang, Q.; Sun, Z.; Wang, J. Synergistic enhancement of thermal conductivity and dielectric properties in Al₂O₃/BaTiO₃/PP composites. *Materials* **2018**, *11*, 1536. [[CrossRef](#)]
8. Fan, L.; Yang, D.; Huang, L.; Fan, M.; Lei, C.; Fu, Q. Polymer nanocomposite with enhanced energy storage capacity by introducing hierarchically-designed 1-dimension hybrid nanofiller. *Polymer* **2020**, *201*, 122608. [[CrossRef](#)]
9. Kuruvilla, S.P.; Renukappa, N.; Rajan, J.S. Influence Hybrid Fillers on Electrical and Mechanical Properties of Fiber Reinforced Epoxy Composites. *Int. J. Eng. Res. Technol. IJERT* **2020**, *9*, 376–383.
10. Navidfar, A.; Trabzon, L. Fabrication and characterization of polyurethane hybrid nanocomposites: Mechanical, thermal, acoustic, and dielectric properties. *Emergent Mater.* **2022**, *5*, 1157–1165. [[CrossRef](#)]
11. Jiang, H.; Zhang, X.; Gao, J.; Guo, N. Conductance Current and Space Charge Characteristics of SiO₂/MMT/LDPE Micro-Nano Composites. *Materials* **2020**, *13*, 4119. [[CrossRef](#)]
12. Hsiao, M.-C.; Ma, C.-C.M.; Chiang, J.-C.; Ho, K.-K.; Chou, T.-Y.; Xie, X.; Tsai, C.-H.; Chang, L.-H.; Hsieh, C.-K. Thermally conductive and electrically insulating epoxy nanocomposites with thermally reduced graphene oxide–silica hybrid nanosheets. *Nanoscale* **2013**, *5*, 5863–5871. [[CrossRef](#)]
13. Osman, A.; Elhakeem, A.; Kaytbay, S.; Ahmed, A. Thermal, electrical and mechanical properties of graphene/nano-alumina/epoxy composites. *Mater. Chem. Phys.* **2021**, *257*, 123809. [[CrossRef](#)]
14. Wang, Y.; Wu, W.; Drummer, D.; Liu, C.; Tomiak, F.; Schneider, K.; Huang, Z. Achieving a 3D thermally conductive while electrically insulating network in polybenzoxazine with a novel hybrid filler composed of boron nitride and carbon nanotubes. *Polymers* **2020**, *12*, 2331. [[CrossRef](#)]
15. Daniel, S.; Thomas, S. Layered double hydroxides: Fundamentals to applications. In *Layered Double Hydroxide Polymer Nanocomposites*; Elsevier: Amsterdam, The Netherlands, 2020; pp. 1–76.
16. Alansi, A.M.; Alkayali, W.Z.; Al-quanaibit, M.H.; Qahtan, T.F.; Saleh, T.A. Synthesis of exfoliated polystyrene/anionic clay MgAl-layered double hydroxide: Structural and thermal properties. *RSC Adv.* **2015**, *5*, 71441–71448. [[CrossRef](#)]
17. Rafiee, F.; Otadi, M.; Goodarzi, V.; Khonakdar, H.A.; Jafari, S.H.; Mardani, E.; Reuter, U. Thermal and dynamic mechanical properties of PP/EVA nanocomposites containing organo-modified layered double hydroxides. *Compos. Part B Eng.* **2016**, *103*, 122–130. [[CrossRef](#)]
18. Ezech, C.I.; Tomatis, M.; Yang, X.; He, J.; Sun, C. Ultrasonic and hydrothermal mediated synthesis routes for functionalized Mg-Al LDH: Comparison study on surface morphology, basic site strength, cyclic sorption efficiency and effectiveness. *Ultrason. Sonochem.* **2018**, *40*, 341–352. [[CrossRef](#)]
19. Li, L.; Qian, Y.; Han, H.; Qiao, P.; Zhang, H. Effects of functional intercalation and surface modification on the flame retardant performance of EVA/LDHs composites. *Polym. Polym. Compos.* **2021**, *29*, 842–853. [[CrossRef](#)]
20. Li, L.; Dai, Y.; Xu, Q.; Zhang, B.; Zhang, F.; You, Y.; Ma, D.; Li, S.-S.; Zhang, Y.-X. Interlayer expanded nickel-iron layered double hydroxide by intercalation with sodium dodecyl sulfate for enhanced oxygen evolution reaction. *J. Alloys Compd.* **2021**, *882*, 160752. [[CrossRef](#)]

21. Alias, A.H.; Norizan, M.N.; Sabaruddin, F.A.; Asyraf, M.R.M.; Norraahim, M.N.F.; Ilyas, A.R.; Kuzmin, A.M.; Rayung, M.; Shazleen, S.S.; Nazrin, A. Hybridization of MMT/Lignocellulosic Fiber Reinforced Polymer Nanocomposites for Structural Applications: A Review. *Coatings* **2021**, *11*, 1355. [[CrossRef](#)]
22. Jose, J.P.; Thomas, S. XLPE based Al₂O₃-clay binary and ternary hybrid nanocomposites: Self-assembly of nanoscale hybrid fillers, polymer chain confinement and transport characteristics. *Phys. Chem. Chem. Phys.* **2014**, *16*, 20190–20201. [[CrossRef](#)] [[PubMed](#)]
23. Mansor, N.; Nazar, N.M.; Ishak, D.; Mariatti, M.; Halim, H.; Basri, A.; Kamarol, M. Study on the Dielectric Performance of XLPE Nanocomposite Against The Electrical Tree Propagation. In Proceedings of the 2020 International Symposium on Electrical Insulating Materials (ISEIM), Tokyo, Japan, 13–17 September 2020; pp. 375–378.
24. Liu, D.; Pourrahimi, A.M.; Olsson, R.T.; Hedenqvist, M.; Gedde, U. Influence of nanoparticle surface treatment on particle dispersion and interfacial adhesion in low-density polyethylene/aluminium oxide nanocomposites. *Eur. Polym. J.* **2015**, *66*, 67–77. [[CrossRef](#)]
25. Ntetsikas, K.; Zapsas, G.; Bilalis, P.; Gnanou, Y.; Feng, X.; Thomas, E.L.; Hadjichristidis, N. Complex star architectures of well-defined polyethylene-based Co/terpolymers. *Macromolecules* **2020**, *53*, 4355–4365. [[CrossRef](#)]
26. Kong, Y.; Huang, Y.; Meng, C.; Zhang, Z. Sodium dodecylsulfate-layered double hydroxide and its use in the adsorption of 17β-estradiol in wastewater. *RSC Adv.* **2018**, *8*, 31440–31454. [[CrossRef](#)]
27. Saman, N.; Awang, N.; Ahmad, M.; Buntat, Z.; Adzis, Z. Partial Discharge Characteristics of Low-Density Polyethylene Nanocomposites Incorporated with Plasma-treated Silica and Boron Nitride Nanofillers. In Proceedings of the 2021 3rd International Conference on High Voltage Engineering and Power Systems (ICHVEPS), Bandung, Indonesia, 5–6 October 2021; pp. 518–523.
28. Lau, K.Y. Structure and Electrical Properties of Silica-Based Polyethylene Nanocomposites. Ph.D. Thesis, University of Southampton, Southampton, UK, 2013.
29. Othman, N.A.; Zainuddin, H.; Aman, A.; Ghani, S.A.; Chairul, I.S. The Correlation between Surface Tracking and Partial Discharge Characteristics on Pressboard Surface Immersed in MIDELE eN. *Int. J. Electr. Comput. Eng.* **2017**, *7*, 631–640. [[CrossRef](#)]
30. Awan, H.A.; Amin, S.; ur Rahman, T.; Asad, U.; Awais, M. Effect of regular and core shell nano fillers on the partial discharge and tracking performance of low density polyethylene. *Mater. Res. Express* **2020**, *7*, 015062. [[CrossRef](#)]
31. Chandrasekar, S.; Purushotham, S.; Montanari, G.C. Investigation of electrical tree growth characteristics in XLPE nanocomposites. *IEEE Trans. Dielectr. Electr. Insul.* **2020**, *27*, 558–564. [[CrossRef](#)]
32. Said, A.R.; Nawar, A.G.; Elsayed, A.; Abd-Allah, M.; Kamel, S. Enhancing Electrical, Thermal, and Mechanical Properties of HV Cross-Linked Polyethylene Insulation Using Silica Nanofillers. *J. Mater. Eng. Perform.* **2021**, *30*, 1796–1807. [[CrossRef](#)]
33. Hoang, A.T.; Serdyuk, Y.V.; Gubanski, S.M. Charge transport in LDPE nanocomposites part II—Computational approach. *Polymers* **2016**, *8*, 103. [[CrossRef](#)]
34. Rafiq, M.; Shafique, M.; Azam, A.; Ateeq, M. The impacts of nanotechnology on the improvement of liquid insulation of transformers: Emerging trends and challenges. *J. Mol. Liq.* **2020**, *302*, 112482. [[CrossRef](#)]
35. Khaled, U.; Beroual, A. AC dielectric strength of mineral oil-based Fe₃O₄ and Al₂O₃ nanofluids. *Energies* **2018**, *11*, 3505. [[CrossRef](#)]
36. Montanari, G.C.; Palmieri, F.; Testa, L.; Motori, A.; Saccani, A.; Patuelli, F. Polarization processes of nanocomposite silicate-EVA and PP materials. *IEEE Trans. Fundam. Mater.* **2006**, *126*, 1090–1096. [[CrossRef](#)]
37. Ashish Sharad, P.; Kumar, K.S. Application of surface-modified XLPE nanocomposites for electrical insulation-partial discharge and morphological study. *Nanocomposites* **2017**, *3*, 30–41. [[CrossRef](#)]
38. Azmi, A.; Lau, K.Y.; Ahmad, N.A.; Abdul-Malek, Z.; Tan, C.W.; Ching, K.Y.; Vaughan, A.S. Structure-dielectric property relationship in polypropylene/multi-element oxide nanocomposites. *IEEE Trans. Nanotechnol.* **2021**, *20*, 377–385. [[CrossRef](#)]
39. Lim, K.S.; Mariatti, M.; Kamarol, M.; Ghani, A.B.A.; Shafi Halim, H.; Abu Bakar, A. Properties of nanofillers/crosslinked polyethylene composites for cable insulation. *J. Vinyl Addit. Technol.* **2019**, *25*, E147–E154. [[CrossRef](#)]
40. Qingyue, Y.; Xiufeng, L.; Peng, Z.; Peijie, Y.; Youfu, C. Properties of Water Tree Growing in XLPE and composites. In Proceedings of the 2019 2nd International Conference on Electrical Materials and Power Equipment (ICEMPE), Guangzhou, China, 7–10 April 2019; pp. 409–412.
41. Sun, K.; Chen, J.; Zhao, H.; Sun, W.; Chen, Y.; Luo, Z. Dynamic thermomechanical analysis on water tree resistance of crosslinked polyethylene. *Materials* **2019**, *12*, 746. [[CrossRef](#)]
42. Thomas, J.; Joseph, B.; Jose, J.P.; Maria, H.J.; Main, P.; Ali Rahman, A.; Francis, B.; Ahmad, Z.; Thomas, S. Recent advances in cross-linked polyethylene-based nanocomposites for high voltage engineering applications: A critical review. *Ind. Eng. Chem. Res.* **2019**, *58*, 20863–20879. [[CrossRef](#)]
43. Lei, M.; Chen, Z.; Lu, H.; Yu, K. Recent progress in shape memory polymer composites: Methods, properties, applications and prospects. *Nanotechnol. Rev.* **2019**, *8*, 327–351. [[CrossRef](#)]
44. Kavitha, D.; Balachandran, M. XLPE-layered silicate nanocomposites for high voltage insulation applications: Dielectric characteristics, treeing behaviour and mechanical properties. *IET Sci. Meas. Technol.* **2019**, *13*, 1019–1025. [[CrossRef](#)]
45. Essawi, S.; Nasrat, L.; Ismail, H.; Asaad, J. Effect of nanoparticles on dielectric, mechanical and thermal characteristics of XLPE/TiO₂ nanocomposites. *Int. J. Adv. Technol. Eng. Explor.* **2021**, *8*, 1243.
46. Srivastava, S.K. Mechanical and dynamical mechanical properties of layered double hydroxide-filled elastomer and elastomeric blend nanocomposites. In *Layered Double Hydroxide Polymer Nanocomposites*; Woodhead Publishing: Sawston, UK, 2020; pp. 347–409.

47. Gill, Y.Q.; Ehsan, H.; Mehmood, U.; Irfan, M.S.; Saeed, F. A novel two-step melt blending method to prepare nano-silanized-silica reinforced crosslinked polyethylene (XLPE) nanocomposites. *Polym. Bull.* **2022**, *79*, 1–17. [[CrossRef](#)]
48. Donghe, D.; Xiufeng, L.; Jin, S.; Peijie, Y.; Youfu, C. The influence of surface modifier on structural morphology and dielectric property of XLPE/SiO₂ nanocomposites. In Proceedings of the 2017 1st International Conference on Electrical Materials and Power Equipment (ICEMPE), Xi'an, China, 14–17 May 2017; pp. 432–435.
49. Wang, S.; Yu, S.; Xiang, J.; Li, J.; Li, S. DC breakdown strength of crosslinked polyethylene based nanocomposites at different temperatures. *IEEE Trans. Dielectr. Electr. Insul.* **2020**, *27*, 482–488. [[CrossRef](#)]
50. Thomas, J.; Thomas, S.; Ahmad, Z. *Crosslinkable Polyethylene Based Blends and Nanocomposites*; Springer: Cham, Switzerland, 2021.

Disclaimer/Publisher's Note: The statements, opinions and data contained in all publications are solely those of the individual author(s) and contributor(s) and not of MDPI and/or the editor(s). MDPI and/or the editor(s) disclaim responsibility for any injury to people or property resulting from any ideas, methods, instructions or products referred to in the content.